Chapter 9
Local Structures, Excited States, and Photocatalytic Reactivities of "Single-Site" Ti-Oxide Photocatalysts Constructed Within Zeolites or Mesoporous Materials

Masaya Matsuoka and Masakazu Anpo

Abstract "Single-site" Ti-oxide species incorporated within the framework or cavities of zeolites as well as mesoporous materials in an isolated state exhibit high and unique photocatalytic activity for various reactions such as the direct decomposition of NO into N_2 and O_2 and the reduction of CO_2 with H_2O to produce CH_4 and CH_3OH. Various in situ spectroscopic investigations using photoluminescence, XAFS (XANES and FT-EXAFS), and ESR techniques revealed that the photo-excited triplet states of the single-site Ti-oxide species play a vital role in these photocatalytic reactions. The photocatalytic activity as well as the selectivity of the Ti-oxide species strongly depends on their local structures. Furthermore, it has been demonstrated that ion-implantation is an effective technique in modifying the electronic properties of single-site Ti-oxide photocatalysts, enabling them to absorb and operate as highly efficient photocatalysts under visible light irradiation ($\lambda > 420$ nm).

1 Introduction

TiO_2 photocatalysts have attracted much attention as unique photo-functional materials enabling effective environmental purification as well as the means for new energy production under UV or solar light irradiation. In fact, semiconducting powdered TiO_2 catalysts have been applied for the decomposition of NO_x in air (Anpo et al. 2005; Anpo and Thomas 2006), the degradation of toxic organic impurities diluted in water (Yamashita et al. 2003), and the decomposition of

M. Anpo (✉)
Department of Applied Chemistry, Graduate School of Engineering,
Osaka Prefecture University, 1-1 Gakuen-cho, Naka-ku, Sakai,
Osaka 599-8531, Japan
e-mail: anpo@chem.osakafu-u.ac.jp

water into H_2 and O_2 (Matsuoka et al. 2007; Kitano et al. 2007). At present, various attempts are being made to enhance the photocatalytic activity of such semiconducting TiO_2 catalysts. One approach is to reduce the particle size of the powdered TiO_2 catalysts. As the size of a TiO_2 particle is reduced below a certain dimension, especially below 100 Å, the energy gap between its highest occupied molecular orbital (HOMO) and lowest unoccupied molecular orbital (LUMO) starts to increase (Fig. 1), leading to an enhancement of the reduction ability of the photo-formed electrons in the LUMO as well as the oxidation ability of the photo-formed holes in the HOMO. This "size quantization effect" is significant when TiO_2 units (Ti-oxide species) are highly dispersed at the molecular level on various metal oxide supports such as zeolites or mesoporous materials with high surface areas (Anpo and Che 2000). In fact, UV irradiation of highly dispersed tetrahedral Ti-oxide species leads to the formation of a charge-transfer excited triplet state involving an electron transfer from O^{2-}(l) to Ti^{4+}(l), which is quite different from the bandgap excitation process which occurs on bulk TiO_2 powders.

$$hv$$

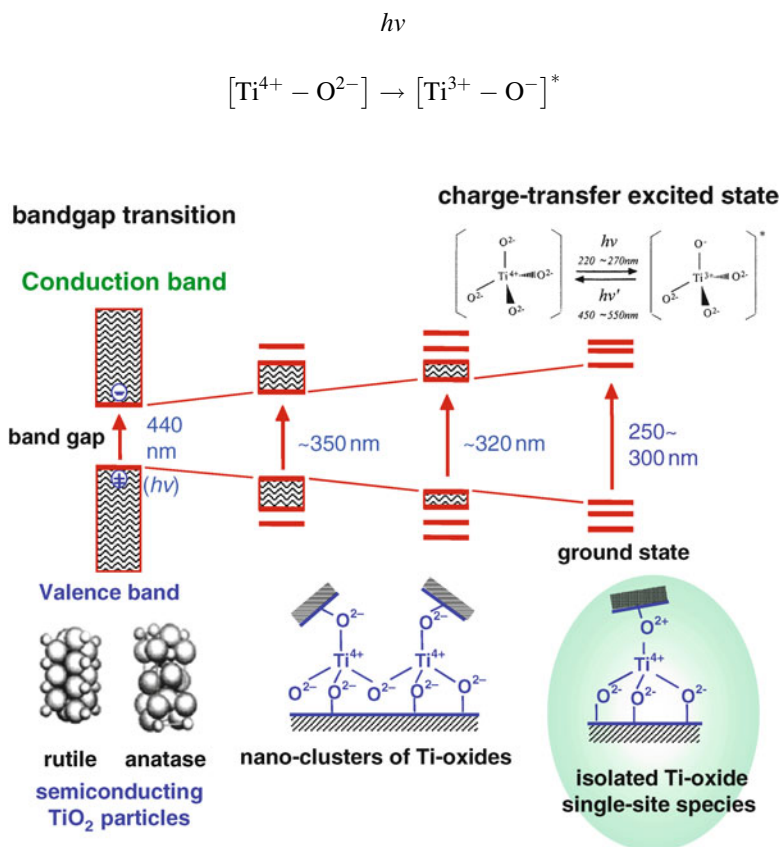$$\left[Ti^{4+} - O^{2-} \right] \rightarrow \left[Ti^{3+} - O^{-} \right]^{*}$$

Fig. 1 Excitation and charge separation of Ti-oxide photocatalysts in molecules, clusters and extended semiconductors

This unique charge-transfer excited triplet state ($[Ti^{3+}–O^-]$*) enables high and selective photocatalytic reactions quite different from photoelectrochemical reactions occurring on bulk TiO_2 powders (Anpo, 2000), due to the close existence of photo-formed electron and hole pairs and their balanced contribution to the reactions. The high reactivity of these charge-transfer excited triplet states can induce various significant photocatalytic reactions such as the decomposition of NO into N_2 and O_2 (Yamashita et al. 1996), the degradation of organic impurities in water (Yamashita et al. 1998), and the reduction of CO_2 with H_2O to produce CH_4 and CH_3OH (Ikeue et al. 2001). These photocatalytic reactions proceed with a high efficiency and selectivity, displaying quite different mechanisms from those observed on semiconducting TiO_2 photocatalysts in which the photoelectrochemical reaction mechanism or charge separation plays an important role. Furthermore, the photocatalytic activity as well as the selectivity of the highly dispersed tetrahedral Ti-oxide species was found to be greatly affected by the various physicochemical properties of the supports, i.e., the hydrophilicity, hydrophobicity, or condensation effect of the gasses for zeolite or mesoporous materials.

In this chapter, we have summarized the photocatalytic activity of single-site Ti-oxide species incorporated into the framework structures or cavities of various zeolites or mesoporous materials at ambient temperatures. The local structures of the Ti-oxide species are discussed based on results obtained by various in situ spectroscopic techniques. Special attention has been focused on the relationship between the local structure of the active sites and their activity for various photocatalytic reactions.

2 Preparation of Ti-Oxide Photocatalysts and Their Local Structures

When the TiO_2 units (Ti-oxide species) are very highly dispersed at the molecular level on various metal oxides supports such as zeolites or mesoporous materials, isolated Ti-oxide species can be formed within the frameworks or cavities of these supports. These Ti-oxide species are regarded as the "single-site" Ti-oxide species since they all exist in a tetrahedral coordination sphere in an isolated state. The introduction of single-site Ti-oxide species within zeolites can be achieved by an ion-exchange method or hydrothermal synthesis. In the case of ion-exchange, zeolites are treated with aqueous solution containing Ti^{4+} ions which are exchanged at the ion-exchange sites on the zeolite framework, i.e., at the Brönsted acid site near the framework aluminum. Ti-oxide-exchanged Y-zeolite (ex-Ti-oxide/Y-zeolite) can be prepared by the ion-exchange of the Y-zeolite ($SiO_2/Al_2O_3 = 5.5$) with an aqueous titanium ammonium oxalate solution (Yamashita and Anpo 2003). On the other hand, hydrothermal synthesis using the precursors silica and titanium oxide and structure directing agents (SDA) enables the direct incorporation of the single-site Ti-oxide species at T-sites within the framework of zeolites in tetrahedral coordination. For example, two types of Ti-oxide containing β-zeolites (Ti-β) with

different affinities to the water molecules can be hydrothermally synthesized by using different SDA having OH^- and F^- as the counter anions. These Ti-β are denoted according to the kind of SDA used, i.e., Ti-β(OH) and Ti-β(F), the former showing more hydrophilic properties than the latter (Yamashita 2002). Another type of single-site Ti-oxide catalyst is mesoporous silica materials containing Ti-oxide species within their amorphous silica wall structure (Ti-MCM-41, Ti-HMS), which can be hydrothermally synthesized or synthesized under ambient conditions using the precursors silica and titanium oxide and template agents.

Figure 2a–e shows the XANES and Fourier transform of EXAFS (FT-EXAFS) for the single-site Ti-oxide catalysts. The XANES for these catalysts showed an intense single preedge peak, indicating that the Ti-oxide species exist in tetrahedral coordination.
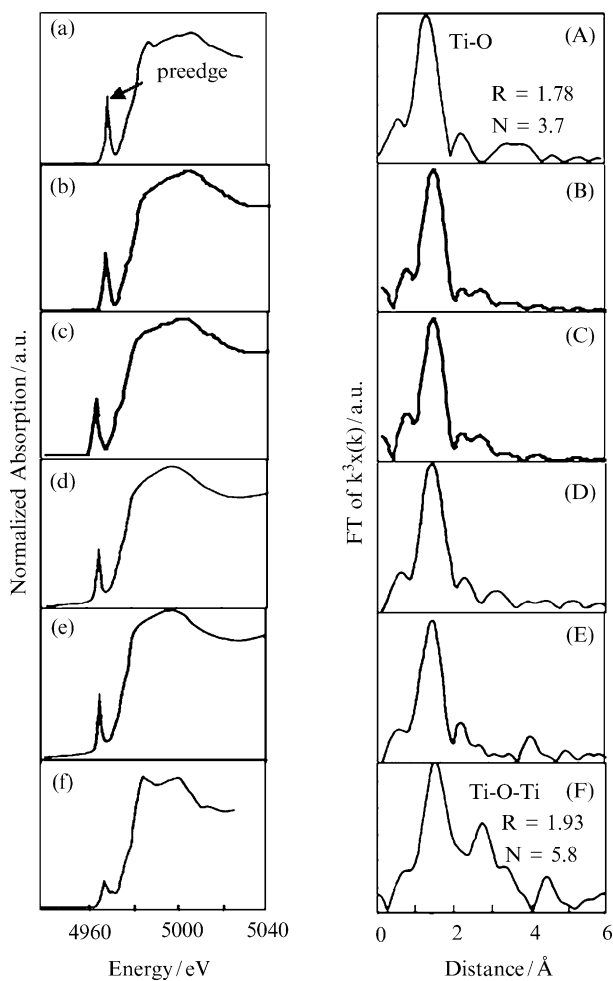

Fig. 2 XANES (*left*) and FT-EXAFS (*right*) spectra of the ex-Ti-oxide/Y-zeolite (**a**, **A**); Ti-β (OH) (**b**, **B**); Ti-β (F) (**c**, **C**); Ti-MCM-41 (**d**, **D**); Ti-HMS (**e**, **E**); and imp-Ti-oxide/Y-zeolite (**f**, **F**)

FT-EXAFS studies showed only a peak assigned to the neighboring oxygen atoms (Ti–O), indicating that the Ti-oxide species exist in an isolated state as "single-site" Ti-oxide species. From curve-fitting analysis of the EXAFS spectra, it was found that the Ti^{4+} ions are surrounded by four oxygen atoms with an atomic distance of around 1.78 Å, showing good agreement with the XANES results (Anpo and Takeuchi 2003). It should also be noted that TiO_2 clusters with small particle sizes can be easily prepared on zeolites or mesoporous silica materials by an impregnation method. As shown in Fig. 2f, the XANES of the Ti-oxide impregnated Y-zeolite (imp-Ti-oxide/Y-zeolite) exhibited a preedge peak which branches off into several distinct weak peaks, showing that the Ti-oxide species exist in octahedral coordination. Furthermore, the FT-EXAFS spectra showed the existence of peaks attributed to the neighboring Ti toms (Ti–O–Ti) in addition to the neighboring O atoms (Ti–O). These results indicate that the Ti-oxide species loaded onto a Y-zeolite by an impregnation method exist in small aggregated TiO_2 clusters. The formation of small aggregated TiO_2 clusters were also observed by XAFS measurements for HMS prepared by an impregnation method (imp-Ti-HMS).

3 Excited States of Ti-oxide Photocatalysts and Their Photocatalytic Reactivities

3.1 Excited States of "Single-Site" Ti-Oxide Species and Their Reactivity

The Ti-oxide species, incorporated within zeolites (ex-Ti-oxide/Y-zeolite, Ti-β (OH), Ti-β(F)), and mesoporous silica (Ti-MCM-41, Ti-HMS) as single-site catalysts, exhibit a UV absorption band at around 230 nm which is attributed to the ligand-to-metal charge transfer transition (LMCT) of the isolated tetrahedral Ti-oxide species involving an electron transfer from the oxygen ligand to the central Ti^{4+} cation (Hu et al. 2006). As shown in Fig. 3, UV irradiation of the absorption band of the single-site Ti-oxide catalysts led to the appearance of a photoluminescence at around 490 nm at 77 K due to the radiative decay process from the charge-transfer excited triplet state to the ground state of the isolated tetrahedral Ti-oxide species, as shown below:

$$(Ti^{4+} - O^{2-}) \underset{h\nu'}{\overset{h\nu}{\rightleftarrows}} (Ti^{3+} - O^-)^*$$
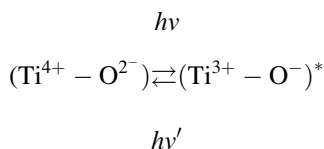
In contrast, the imp-Ti-oxide/Y-zeolite and imp-Ti-HMS catalysts did not exhibit any photoluminescence. Thus, these results clearly indicate that Ti-oxide catalysts prepared by an impregnation method involving the aggregated octahedral Ti-oxide
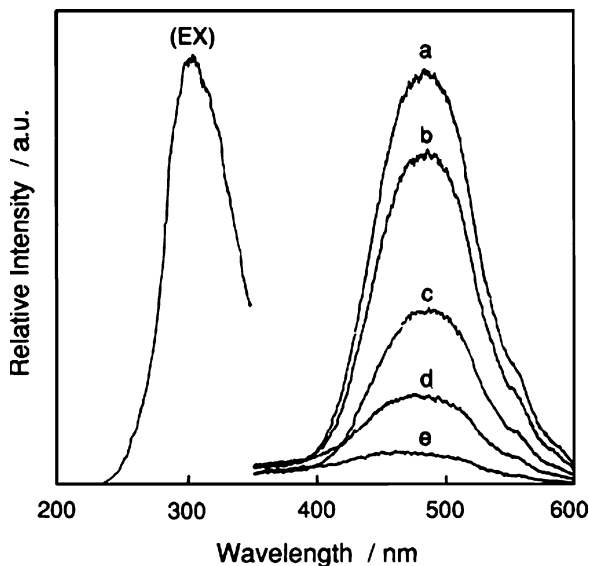
Fig. 3 Photoluminescence spectrum of the ex-Ti-oxide/Y-zeolite catalyst (**a**); its excitation spectrum (EX); and the effect of the addition of NO on the photoluminescence spectrum (**b–e**). Measured at 77 K; excitation beam: 290 nm; emission monitored at 490 nm; amounts of added NO: (**a**) 0.0, (**b**) 0.2, (**c**) 0.8, (**d**) 7.6, (**e**) 21.3 μmol/g

species do not exhibit any photoluminescence spectrum. The reactivity of the single-site Ti-oxide species in its photo-excited state has also been investigated by photoluminescence quenching measurements. The addition of various gasses such as NO, CO_2, and H_2O on single-site Ti-oxide catalysts (ex-Ti-oxide/Y-zeolite) led to an efficient quenching of the photoluminescence (Fig. 3). The lifetime of the charge transfer excited triplet state of the single-site Ti-oxide species was also shortened by the addition of these gasses, its extent depending on the amount of gasses added. Such an efficient quenching of the photoluminescence suggests not only that the tetrahedrally coordinated Ti-oxide species is located at positions accessible to the added gasses but also that the gasses interact and/or react with the single-site Ti-oxide species in their excited triplet states.

3.2 Photocatalytic Decomposition of NO on Single-Site Ti-Oxide Photocatalysts

Nitric oxide (NO) is an especially harmful atmospheric pollutant and the main cause of acid rain and photochemical smog, which is emitted largely from the reaction of N_2 with O_2 in high-temperature combustion processes. It has been reported that Ti-oxide photocatalysts can be applied for the clean, safe, and low-temperature removal of NO. UV irradiation of single-site Ti-oxide photocatalysts in the presence of NO efficiently led to the formation of N_2 and O_2 as major products with a good linearity against the UV irradiation time, as shown in Fig. 4. The formation of N_2O

was observed only as a minor product. On the other hand, when the powdered TiO_2 or imp-Ti-oxide/Y-zeolite loaded with small Ti-oxide clusters was applied as a photocatalyst for the decomposition of NO, the major products formed were N_2O and NO_2 (Zhang et al. 2001). Thus, the efficiency and selectivity for the formation of N_2 strongly depend on the type of catalysts. Figure 4 shows the relationship between the coordination number of the Ti-oxide species and the selectivity for N_2 formation in the photocatalytic decomposition of NO on various Ti-oxide photocatalysts. A clear dependence of the N_2 selectivity on the coordination number of the Ti-oxide species can be observed, i.e., the lower the coordination number of the Ti-oxide species, the higher the N_2 selectivity. From these results, a highly efficient and selective photocatalytic reduction of NO into N_2 and O_2 was found to be achieved using single-site Ti-oxide catalysts involving highly dispersed, isolated tetrahedral Ti-oxides as the active species. The formation of N_2O as the major product was observed for bulk TiO_2 catalysts and on imp-Ti-oxide/Y-zeolite catalysts involving aggregated octahedrally-coordinated Ti-oxide species.

From the investigations of these photocatalytic reactions as well as the quenching of the photoluminescence, the reaction mechanism for the photocatalytic decomposition of NO on the isolated tetrahedral titanium oxide species can be proposed, as shown in Scheme 1. The NO species are able to adsorb onto single-site Ti-oxide species as weak ligands to form the reaction precursors. Under UV
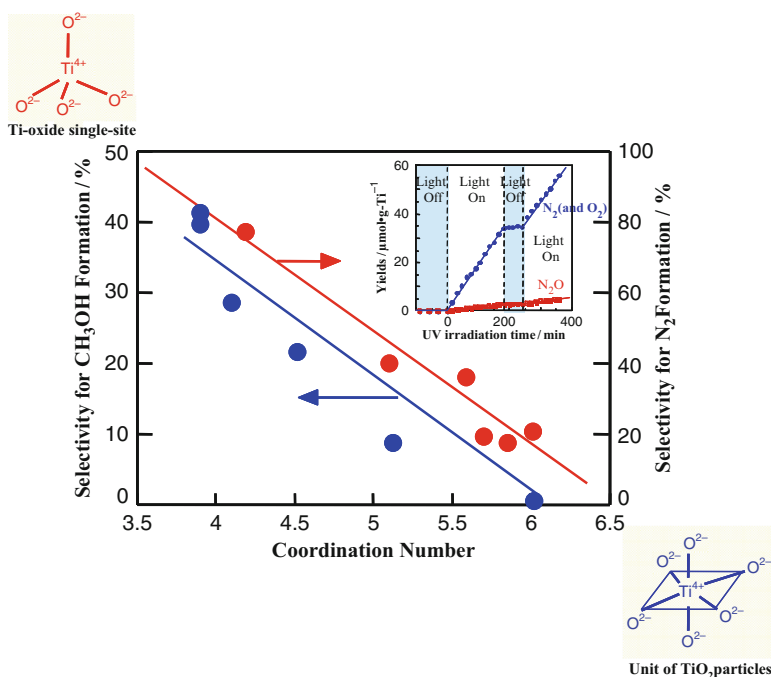

Fig. 4 Relationship between the coordination numbers and the photocatalytic reactivity of the titanium oxides. *Figure inset*: Time profiles of the photocatalytic decomposition of NO into N_2 and N_2O on the Ti-oxide/Y-zeolite catalyst

irradiation, the charge-transfer excited complexes of Ti-oxide species $(Ti^{3+}-O^-)^*$ are formed. Within their lifetimes, the electron transfer from the trapped electron center, Ti^{3+}, into the π-antibonding orbital of NO takes place. Simultaneously, the electron transfer from the π-bonding orbital of another NO into the trapped hole center, O^-, occurs. These electron transfers led to the direct decomposition of two sets of NO on $(Ti^{3+}-O^-)^*$ into N_2 and O_2 under UV irradiation in the presence of NO even at 275 K. On the other hand, with the aggregated or bulk TiO_2 catalysts, the photo-formed holes and electrons rapidly separate from each other with large space distances between the holes and electrons, thus preventing the simultaneous activation of two NO molecules on the same active sites and resulting in the formation of N_2O and NO_2 in place of N_2 and O_2. The decomposed N and O species react with NO on different sites to form N_2O and NO_2, respectively.

3.3 Photocatalytic Reduction of CO_2 with H_2O on Single-Site Ti-Oxide Photocatalysts

Photocatalysis for the reduction of CO_2 with H_2O is of interest not only as a reaction system utilizing artificial photosynthesis but as a way to use carbon sources for the synthesis of hydrocarbons and oxygenate such as CH_4 and CH_3OH. In this reaction, photon energy is converted into chemical energy and stored in the bonds of CH_4 and
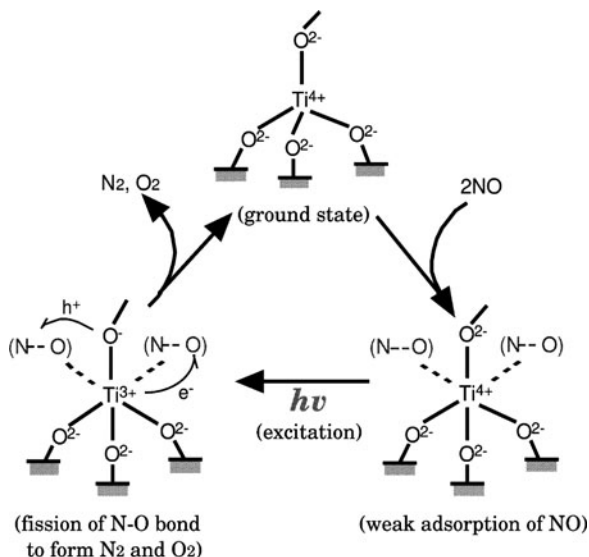
Scheme 1 The reaction mechanism of the photocatalytic decomposition of NO into N_2 and O_2 on the tetrahedrally-coordinated Ti-oxide species under UV light irradiation

CH_3OH, accompanied by a large positive change in the Gibbs free energy ($\Delta G > 0$). It has previously been reported that the photocatalytic reduction of CO_2 with H_2O proceeds efficiently on single-site Ti-oxide photocatalysts (Shioya et al. 2003). UV irradiation of powdered TiO_2 and Ti-oxide/Y-zeolite catalysts prepared by ion-exchange or impregnation methods in the presence of a mixture of CO_2 and H_2O led to the evolution of CH_4 and CH_3OH in the gas phase at 328 K, as well as trace amounts of CO, C_2H_4, and C_2H_6. The evolution of small amounts of O_2 was also observed. It can be seen that the specific photocatalytic reactivity of the Ti-oxide/Y-zeolite catalysts, which have been normalized by unit gram of Ti in the catalysts, is much higher than bulk TiO_2. The ex-Ti-oxide/Y-zeolite exhibits a high reactivity and selectivity for the formation of CH_3OH, while the formation of CH_4 was found to be the major reaction on bulk TiO_2 as well as on the imp-Ti-oxide/Y-zeolite. A clear relationship between the coordination number of the Ti-oxide species and the selectivity for CH_3OH formation can be observed (Fig. 4), showing that the highly efficient, highly selective photocatalytic reduction of CO_2 with H_2O into CH_3OH can be achieved using the single-site Ti-oxide catalysts such as ex-Ti-oxide/Y-zeolite, which includes the highly dispersed isolated tetrahedral Ti-oxide as the active species. Furthermore, the reaction selectivity was shown to be greatly dependent on the hydrophilicity of single-site Ti-oxide catalysts. As shown in Fig. 5, two kinds of Ti-β catalysts, [Ti-β(OH), Ti-β(F)], i.e., single-site Ti-oxide photocatalysts, exhibited different adsorption isotherms, Ti-β(OH) showing much higher affinity to the H_2O molecules than Ti-β(F). Figure 6 shows the effect of the addition of H_2O on the preedge peak of the XANES spectrum of the Ti-β catalysts [Ti-β(OH), Ti-β(F)] (Yamashita et al. 2002). It has been established that when the coordination number of the Ti-oxide species increases, the intensity of the preedge peak decreases accompanied by a shift in the preedge peak to higher energy regions. The changes in the peak intensity and position upon H_2O addition are more remarkable for Ti-β(OH) than for Ti-β(F), indicating that the isolated tetrahedral Ti-oxide species within Ti-β(OH) can interact more efficiently with the H_2O molecules. As shown in Fig. 7, the photocatalytic reduction of CO_2 with H_2O proceeds with different reactivities and selectivities on hydrophilic Ti-β(OH) and hydrophobic Ti-β(F). The higher reactivity for the formation of CH_4 observed for Ti-β(OH) and the higher selectivity for the formation of CH_3OH observed for Ti-β(F) may be attributed to the different affinities of the zeolite pores on the H_2O molecules. These results suggest that the hydrophilic–hydrophobic property of zeolite cavities is one of the most important factor to determine the selectivity in the photocatalytic reduction of CO_2 with H_2O.

The reaction mechanism of photocatalytic reduction of CO_2 with H_2O was investigated by photoluminescence and ESR investigations. The addition of H_2O or CO_2 molecules to the ex-Ti-oxide/Y-zeolite led to an efficient quenching of the photoluminescence as well as a shortening of the photoluminescence lifetime, indicating that the added CO_2 or H_2O interacts and/or reacts with the single-site Ti-oxide species in both its ground and excited states.

It was also found that UV irradiation of the single-site Ti-oxide species in the presence of CO_2 and H_2O at 77 K led to the appearance of ESR signals due to the Ti^{3+} ions, H atoms, and carbon radicals (Anpo and Chiba 1992). From these
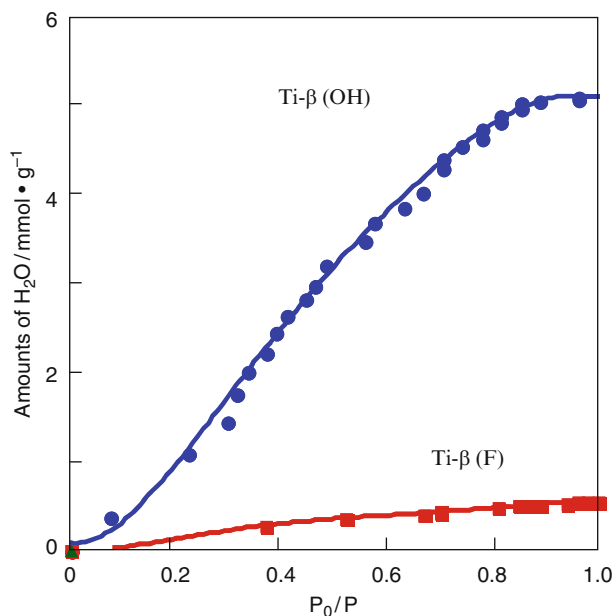
Fig. 5 H_2O adsorption isotherms at 298 K for (**a**) Ti-β(OH) and (**b**) Ti-β(F)

results, the following reaction could be proposed: CO_2 and H_2O molecules interact with the photo-excited Ti-oxide species $(Ti^{3+}–O^-)^*$ and the reduction of CO_2 and the decomposition of H_2O proceed competitively. Furthermore, H atoms and $OH^{\cdot}$ radicals are formed from the H_2O and react with the carbon species formed from CO_2 to produce CH_4 and CH_3OH. These results clearly demonstrate that single-site Ti-oxide photocatalysts within zeolite cavities are applicable as effective photocatalysts enabling artificial photosynthetic reactions such as CO_2 fixation with H_2O to produce CH_3OH with a high selectivity.

3.4 Photocatalytic Size-Screening Oxidation of Organic Compounds on Single-Site Ti-Oxide Catalysts Incorporated Within the Framework of Titanosilicate Molecular Sieves

Recently, Shiraishi et al. (2005) have reported that titanosilicate molecular sieves, when activated by UV irradiation in water in the presence of molecular oxygen, can catalyze oxidative conversions of molecules with a similar size as the pore size of the catalysts but are inactive for much larger or smaller sizes. In other words, titanosilicate molecular sieves act as unique "size-screening" photocatalysts. Photocatalytic oxidative conversions of 25 kinds of phenol derivatives have been investigated on titanosilicate molecular sieves (TS-1 and TS-2), TiO_2, and Ti-SiO_2
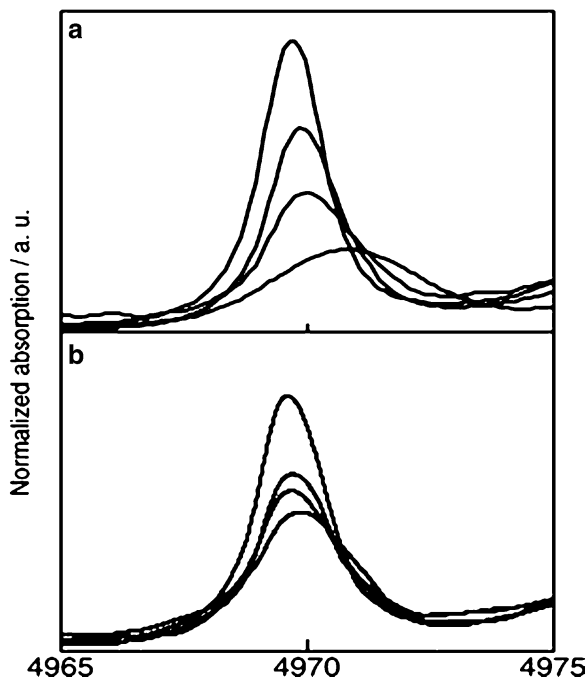
Fig. 6 The effect of the addition of H_2O molecules on the intensity and position of the preedge peak observed in the Ti K-edge XANES spectra of: (**a**) Ti-β(OH) and (**b**) Ti-β(F). Amount of added H_2O molecules: 0, 1.4, 3.0, and 4.6 mmol/g cat (*from top to bottom*)

catalysts under photo-irradiation ($\lambda > 280$ nm; 0.5 h) in the presence of water and O_2. Here, TS-1 and TS-2, both containing 0.4 mol % Ti (= Ti/(Ti + Si) ratio), were prepared by hydrothermal synthesis. Ti-SiO$_2$ having an amorphous structure and containing 0.4 mol % Ti was prepared by a sol–gel method. UV–Vis investigations suggested that highly dispersed "single-site" tetrahedral Ti-oxide species exist within the titanosilicate molecular sieves (TS-1 and TS-2) and Ti-SiO$_2$ catalysts as active species. Furthermore, XRD studies showed that TS-1 has a MFI structure with pore dimensions of 0.54×0.56 nm (sinusoid channel) and 0.52×0.58 nm (straight channel), while TS-2 has a MEL structure with pore dimensions of 0.53×0.54 nm. Photocatalytic oxidative conversions of phenol derivatives on TS-2 were also examined. The close relationship between the effective molecular width (EMW) of the phenol derivatives and their oxidative conversions was observed. The conversion of phenol derivatives with EMW of less than 0.55 nm was nearly zero, however, obviously higher for derivatives with EMW of 0.6–0.65 nm, which is 12–21% larger than the average pore diameter of TS-2 (0.535 nm). Moreover, conversions of the phenol derivatives with EMW of larger than 0.68 nm were found to be almost zero. Similar results have been obtained for reactions on TS-1. In contrast, no EMW-dependent profile was observed for bulk TiO$_2$ or Ti-SiO$_2$ having no micropore structures, while conversions of phenol
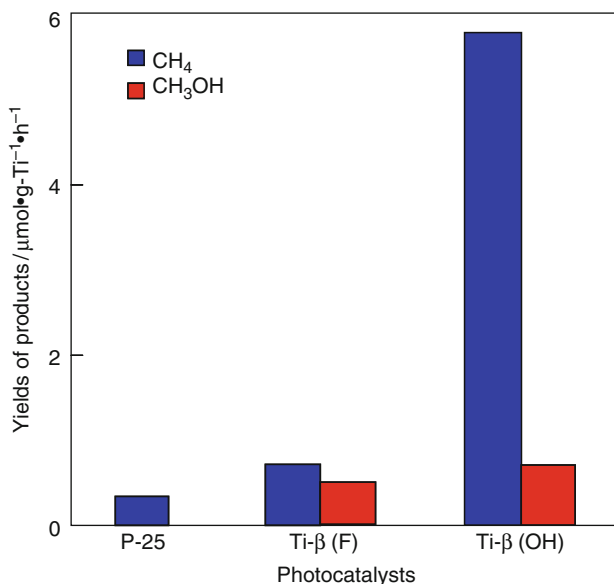
Fig. 7 Yields of CH_4 and CH_3OH in the photocatalytic reduction of CO_2 with H_2O at 323 K on the Ti-β(OH), Ti-β(F), and TiO_2 (P-25) catalysts

derivatives on Ti-SiO_2 was found to be negligible, independent of the EMW of phenol derivatives. From these results, the following mechanism could be proposed for the size-screening oxidation activity of TS-1 and TS-2: The lifetime of the photo-excited state of the single-site tetrahedral Ti-oxide species $[Ti^{3+}–O^-]^*$ is shortened significantly in the presence of H_2O, a strong quencher. A slim molecule having rather small EMW than the pore diameter of the catalyst diffuses smoothly inside the pore and can barely be trapped by the short-lived $[Ti^{3+}–O^-]^*$. In contrast, the diffusion of a molecule with a size close to that of the pore is restricted by the pore wall, and such an "interlocked" molecule is trapped easily by $[Ti^{3+}–O^-]^*$, resulting in high conversion. Considering that the zeolite framework is distorted in solution and the pore structure changes elastically, molecules of ca. 10–20% larger EMW than that of the pore may be interlocked more easily, allowing for, especially, high conversion. Zero conversion of phenol derivatives on Ti-SiO_2 is, therefore, attributed to the lack of pores that regulate the motion of the phenol derivatives. Such catalytic properties demonstrate the potential use of the catalyst for the selective transformation of molecules associated with size reduction, i.e., the "molecular shave" transformation.

The molecular shave transformation, induced by titanosilicate molecular sieves, was examined by the selective transformation of 2-chlorohydroquinone. The EMW of 2-chlorohydroquinone (0.6149 nm) was 12 and 15% larger than the TS-1 and TS-2 pores, respectively, thus allowing the effective photoconversion of 2-chlorohydroquinone into 1,2,4-trihydroxybenzene on both catalysts with high conversion (>67%) and high selectivity (>85%). This high selectivity can be

ascribed to the relatively smooth diffusion of 1,2,4-trihydroxybenzene (EMW: 0.5762 nm) inside the pores of the catalysts as compared to 2-chlorohydroquinone, which prevents the further oxidation of 1,2,4-trihydroxybenzene. In fact, photo-irradiation of bulk TiO_2 in the presence of 2-chlorohydroquinone led to the formation of 1,2,4-trihydroxybenzene as the initial product, while its yield was quite low (1%) since the sequential oxidative decomposition of 1,2,4-trihydroxybenzene proceeds efficiently on TiO_2. These results demonstrate that the molecular shave catalytic system enables the detoxification of chlorophenols and the synthesis of valuable phenol derivatives all at once, proving that this "green" photocatalyst may contribute to the development of economically and environmentally friendly chemical processes.

3.5 Design and Development of Visible-Light-Responsive Single-Site Ti-Oxide Photocatalysts

It has been shown that single-site Ti-oxide photocatalysts anchored within various zeolites or mesoporous silica support exhibit unique and high photocatalytic activity for various reactions such as the direct decomposition of NO into N_2 and O_2 or the reduction of CO_2 with H_2O. In fact, the isolated tetrahedral Ti-oxide species, the active site of the single-site Ti-oxide photocatalyst, can absorb UV light of wavelengths below 300 nm, since the HOMO–LUMO energy gap of the isolated tetrahedral Ti-oxide species becomes significantly larger than that of bulk TiO_2 due to the size quantization effect. However, single-site Ti-oxide photocatalysts which can operate efficiently under both UV and visible light irradiation would be ideal for practical and widespread use. Recently, Anpo et al. (2002) have applied a metal-ion-implantation method to modify the electronic properties of single-site Ti-oxide photocatalysts by bombarding them with high-energy metal ions, showing that metal ion-implantation with various transition metal ions such as V or Cr accelerated by high electric fields produces a large shift in the absorption band of the photocatalyst toward visible light regions. As shown in Fig. 8, the absorption spectra of Ti-HMS at around 200–260 nm, due to the tetrahedral single-site Ti-oxide species, shift smoothly toward visible light regions after V ion implantation, the extent of the shift strongly depending on the amount of V ions implanted. In order to investigate the interactions between the tetrahedral single-site Ti-oxide species and the implanted V ions, EXAFS measurements were carried out. The V K-edge FT-EXAFS spectra of the Ti-HMS catalyst implanted with V ions exhibited a peak due to the V–O–Ti bond, suggesting the direct interaction between the tetrahedral Ti-oxide species and implanted V ions. These findings show that the formation of V–O–Ti bridge structures between the isolated tetrahedral TiO_4 unit and implanted V ions affect the electronic structure of the single-site Ti-oxide species, leading to a red shift in the absorption spectra of these catalysts.

The photocatalytic activity of the V ion-implanted Ti-HMS (V-Ti-HMS) has been investigated for the decomposition of NO into N_2 and O_2 under visible light
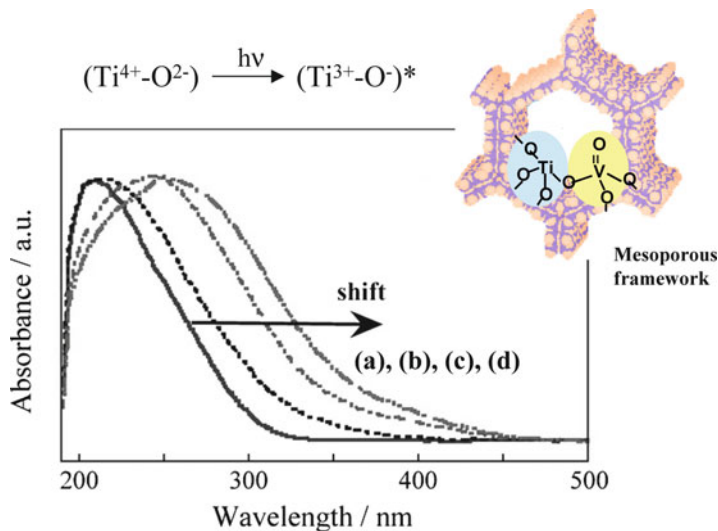
Fig. 8 The diffuse reflectance UV–Vis absorption spectra of V-Ti-HMS. The amount of implanted V ions (μmol/g-cat): (**a**) 0, (**b**) 0.66, (**c**) 1.3, and (**d**) 2.0
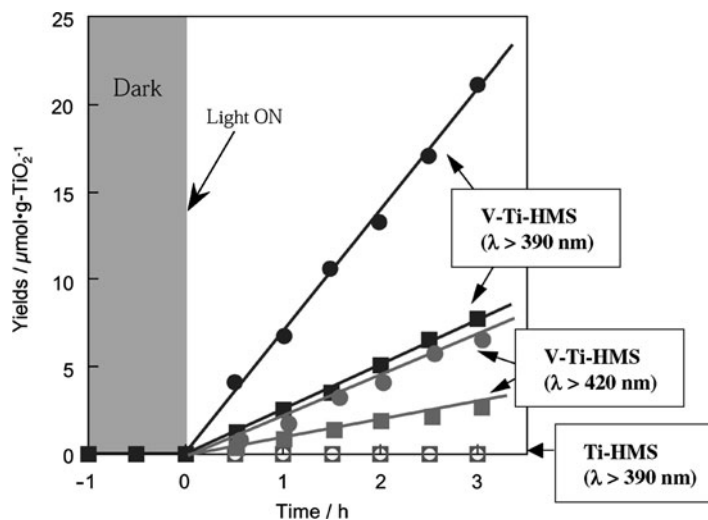

Fig. 9 Time profiles of the photocatalytic decomposition of NO into N_2( ) and N_2O( ) on the V-Ti-HMS and Ti-HMS catalysts

irradiation ($\lambda > 420$ nm). As shown in Fig. 9, visible light irradiation of V-Ti-HMS led to the efficient decomposition of NO into N_2 and O_2, while the unimplanted original Ti-HMS exhibited no activity for the reaction under the same reaction conditions. It was also confirmed that NO decomposition did not proceed at all under UV ($\lambda < 300$ nm) or visible light irradiation ($\lambda > 420$ nm) on the

V ion-implanted HMS without Ti. These results clearly show that ion-implantation is an effective technique in modifying the electronic properties of single-site Ti-oxide photocatalysts, enabling them to absorb and operate as highly efficient photocatalysts under visible light irradiation ($\lambda > 420$ nm).

4   Summary

In this chapter, the local structures of the single-site Ti-oxide species incorporated into the zeolite framework or cavities as well as into the wall structure of mesoporous silica were discussed based on results of such in situ spectroscopic techniques as ESR, UV–Vis, photoluminescence, and XAFS (XANES and FT-EXAFS). The interactions of these active species with gaseous NO and CO_2 were investigated along with the photocatalytic reactivity of the catalysts for the decomposition of NO as well as the reduction of CO_2 with H_2O.

The Ti-oxide species, which are incorporated into the frameworks or cavities of various zeolites or mesoporous silica by ion-exchange or hydrothermal synthesis, were found to exist in highly dispersed tetrahedral coordination states and to act as efficient photocatalysts for the decomposition of NO into N_2 and O_2 as well as the reduction of CO_2 with H_2O to produce CH_4 and CH_3OH. Photoluminescence investigations revealed that the efficient interactions of the charge-transfer excited complexes of the single-site Ti-oxides $(Ti^{3+}–O^-)^*$ i.e., the electron–hole pair state with such reactant molecules as NO, CO_2, and H_2O, play a significant role in these photocatalytic reactions. The localized excitation of the single-site Ti-oxide species led to unique photocatalytic properties quite different from those of semiconducting powdered TiO_2 photocatalysts. It was also demonstrated that single-site Ti-oxide catalysts such as TS-1 can induce the size-screening oxidation of phenols, enabling the detoxification of chlorophenols and the synthesis of valuable phenol derivatives. Thus, by utilizing zeolites or mesoporous silica as a support, it was possible to control the local structure of the highly dispersed Ti-oxide species at an atomic level, leading to the precise control of the photocatalytic activity as well as selectivity of a reaction. Furthermore, the ion-implantation method described here has been shown to be effective in preparing visible light-responsive Ti-oxide photocatalysts involving zeolitic or mesoporous silica frameworks for the development of efficient systems to reduce or eliminate global air and water pollution even under visible or solar light irradiation.

References

Anpo M (ed) (2000) Photofunctional zeolites, NOVA Publishers Inc., and references therein

Anpo M, Che M (2000) Applications of photoluminescence techniques to the characterization of solid surfaces in relation to adsorption, catalysis, and photocatalysis. Adv Catal 44:119–257

Anpo M, Chiba K (1992) Photocatalytic reduction of CO_2 on anchored titanium-oxide catalysts. J Mol Catal 74:207–212

Anpo M, Takeuchi M (2003) The design and development of highly reactive titanium oxide photocatalysts operating under visible light irradiation. J Catal 216:505–516

Anpo M, Thomas JM (2006) Single-site photocatalytic solids for the decomposition of undesirable molecules. *Chem Commun*, 3273–3278

Anpo M, Takeuchi M, Ikeue K, Doshi S (2002) Design and development of titanium oxide photocatalysts operating under visible and UV light irradiation. The applications of metal ion-implantation techniques to semiconducting TiO_2 and Ti/zeolite catalysts. Curr Opin Solid State Mater Sci 6:381–388

Anpo M, Dohshi S, Kitano M, Hu Y, Takeuchi M, Matsuoka M (2005) The preparation and characterization of highly efficient titanium oxide-based photofunctional materials. Ann Rev Mater Res 35:1–27

Hu Y, Martra G, Zhang JL, Higashimoto S, Coluccia S, Anpo M (2006) Characterization of the local structures of Ti-MCM-41 and their photocatalytic reactivity for the decomposition of NO into N_2 and O_2. J Phys Chem B 110:1680–1685

Ikeue K, Yamashita H, Anpo M, Takewaki T (2001) Photocatalytic reduction of CO_2 with H_2O on Ti-beta zeolite Photocatalysts: effect of the hydrophobic and hydrophilic properties. J Phys Chem B 105:8350–8355

Kitano M, Takeuchi M, Matsuoka M, Thomas JM, Anpo M (2007) Photocatalytic water splitting using Pt-loaded visible light-responsive TiO_2 thin film photocatalysts. Catal Today 120:133–138

Matsuoka M, Kitano M, Takeuchi M, Tsujimaru K, Anpo M, Thomas JM (2007) Photocatalysis for new energy production – recent advances in photocatalytic water splitting reactions for hydrogen production. Catal Today 122:51–61

Shioya Y, Ikeue K, Ogawa M, Anpo M (2003) Synthesis of transparent Ti-containing mesoporous silica thin film materials and their unique photocatalytic activity for the reduction of CO_2 with H_2O. Appl Catal A – General 254:251–259

Shiraishi Y, Saito N, Hirai T (2005) Titanosilicate molecular sieve for size-screening photocatalytic conversion. J Am Chem Soc 127:8304–8306

Yamashita H, Anpo M (2003) Local structures and photocatalytic reactivities of the titanium oxide and chromium oxide species incorporated within micro- and mesoporous zeolite materials: XAFS and photoluminescence studies. Curr Opin Solid State Mater Sci 7:471–481

Yamashita H, Ichihashi Y, Anpo M, Hashimoto M, Louis C, Che M (1996) Photocatalytic decomposition of NO at 275 K on titanium oxides included within Y-zeolite cavities: the structure and role of the active sites. J Phys Chem B 100:16041–16044

Yamashita H, Kawasaki S, Ichihashi Y, Harada M, Takeuchi M, Anpo M, Stewart G, Fox MA, Louis C, Che M (1998) Characterization of titanium-silicon binary oxide catalysts prepared by the sol-gel method and their photocatalytic reactivity for the liquid-phase oxidation of 1-octanol. J Phys Chem B 102:5870–5875

Yamashita H, Ikeue K, Takewaki T, Anpo M (2002) In situ XAFS studies on the effects of the hydrophobic-hydrophilic properties of Ti-beta zeolites in the photocatalytic reduction of CO_2 with H_2O. Topic Catal 18:95–100

Yamashita H, Harada M, Misaka J, Takeuchi M, Neppolian B, Anpo M (2003) Photocatalytic degradation of organic compounds diluted in water using visible light-responsive metal ion-implanted TiO_2 catalysts: Fe ion-implanted TiO_2. Catal Today 84:191–196

Zhang JL, Hu Y, Matsuoka M, Yamashita H, Minagawa M, Hidaka H, Anpo M (2001) Relationship between the local structures of titanium oxide photocatalysts and their reactivities in the decomposition of NO. J Phys Chem B 105:8395–8398